https://doi.org/10.5194/egusphere-2026-353
Preprint. Discussion started: 28 January 2026
© Author(s) 2026. CC BY 4.0 License.

Regional contrasts of ecosystem productivity sensitivity to atmospheric CO_2 growth across East Asia

Yun-Soo Na[1], Sang-Wook Yeh[1], Jong-Seong Kug[2]

[1]Department of Marine Science and Convergence Engineering, Hanyang University, ERICA, Ansan, South Korea
[2]School of Earth and Environmental Sciences, Seoul National University, Seoul, South Korea

Correspondence to: Sang-Wook Yeh (swyeh@hanyang.ac.kr)

Abstract. Elevated global atmospheric CO_2 intensifies the complexity of climate variability and ecosystem productivity, and its impact on terrestrial ecosystems carbon cycle remains unclear. Using twelve Dynamic Global Vegetation Models (DGVMs) in Trends in land carbon cycle datasets and Global Carbon Budget dataset, we quantified the sensitivity of ecosystem productivity-defined as the rate of change in productivity with global atmospheric CO_2 growth rate-in East Asia from 1959 to 2023. Most DGVMs showed net ecosystem production sensitivity as negative, implying a weakening of terrestrial carbon absorption capacity in response to elevated atmospheric CO_2. By separating East Asia into monsoon and non-monsoon regions, we examined the temporal changes in gross primary productivity sensitivity, which has been decreasing in both regions since the late 1990s. These productivity responses were primarily controlled by soil moisture sensitivity in non-monsoon region, whereas photosynthetically active radiation emerged as the key factor in monsoon region. Furthermore, the dominance of croplands and woody savannas in monsoon region contributes to regional difference in the mechanism associated with vegetation productivity to atmospheric CO_2 growth. By considering regional climate systems and vegetation characteristics, this study highlights that environmental and structural differences influence the ecosystem response to atmospheric CO_2 growth. Ultimately, our findings suggest that considering regionally distinct climate-vegetation feedbacks is essential for improving the accuracy of global carbon cycle projections under future climate change.

1 Introduction

Assessing terrestrial ecosystems response to rising atmospheric CO_2 is crucial for understanding future vegetation-carbon-climate feedback. Terrestrial ecosystems act as a major carbon sink, with vegetation absorbing 112-169 PgC/year through photosynthesis (Penuelas, 2023; Baldocchi et al., 2016). The carbon absorption through photosynthesis of such vegetation varies by region and seasonality (Na and Yeh, 2025; Bi et al., 2022; Ueyama et al., 2024). While ecosystem productivity can be enhanced by the CO_2 fertilization effect as atmospheric CO_2 increases in response to climate change, it can also be weakened by climate variability such as temperature and respiration (Yun et al., 2022). In particular, East Asia exhibits contrasting precipitation patterns and vegetation characteristics across the region (Fu, 2003; He et al., 2022b; Kim and Park, 2016), where a greater diversity of factors interact to regulate ecosystem carbon exchange.

https://doi.org/10.5194/egusphere-2026-353
Preprint. Discussion started: 28 January 2026
© Author(s) 2026. CC BY 4.0 License.

Numerous studies have analyzed regional and temporal variations in gross primary productivity (GPP), i.e., the carbon uptake by vegetation through photosynthesis in terrestrial ecosystems. While increases in atmospheric CO_2 generally enhance vegetation productivity through photosynthesis, this effect has been weakening in recent decades (Wang et al., 2020) despite that the atmospheric CO_2 growth rate (ACGR, hereafter), which is defined as the year-to-year increase in global atmospheric CO_2 concentration, has rapidly increased (Canadell et al., 2007; Friedlingstein et al., 2024). In addition, the strong positive effect of CO_2 on GPP has diminished to nearly half since the 2000s, with the extent of this reduction varying across climate zones (Wang et al., 2024). Another study analyzing decadal-scale changes in factors affecting global GPP and vegetation activity found that GPP showed the strongest correlations with photosynthetically active radiation (PAR), temperature, and vapor pressure deficit over time, revealing temporal variability in these relationships (Shin et al., 2025; Madani et al., 2020).

In East Asia, links between the East Asian Summer Monsoon and GPP have also been suggested. For example, changes in atmospheric circulation field, precipitation, and downward solar radiation associated with the East Asian summer monsoon result in regional differences in GPP within China (Han et al., 2024). However, research comparing the key environmental factors influencing GPP sensitivity-defined as the response of vegetation productivity to variations in the ACGR-between monsoon and other regions is not well organized. Building upon these findings, this study investigates the primary drivers of changes in GPP sensitivity to ACGR in East Asia.

We provide the sensitivity of terrestrial ecosystem productivity in East Asia to global ACGR using Dynamic Global Vegetation Models (DGVMs) in Trends in land carbon cycle (TRENDY) datasets and Global Carbon Budget dataset. By contrasting GPP changes in monsoon and non-monsoon regions in East Asia and examining relevant environmental factors such as soil moisture (SM) and PAR, we aim to identify mechanisms explaining regional differences in the sensitivity of terrestrial ecosystem productivity to global ACGR in East Asia. Understanding these regional differences can improve the projection of future vegetation-carbon-climate feedback in East Asia.

2 Data and Methods

2.1 Atmospheric CO_2 growth rate

We used global ACGR from 1959 to 2023 from the Global Carbon Budget 2024, provided by the US National Oceanic and Atmospheric Administration Global Monitoring Laboratory (Lan et al., 2025). Data from 1959 to 1979 are observed by the Scripps Institution of Oceanography, based on average atmospheric CO_2 concentration measured at Mauna Loa and South Pole stations (Keeling et al., 1976). Data from 1980 to 2023 are estimated from global averages of multiple stations (Global Carbon Project, 2024). The ACGR was calculated as the annual change in atmospheric CO_2 concentration, defined as the year-to-year difference [GtC yr^{-1}] (Global Carbon Project, 2024; Friedlingstein et al., 2024).

https://doi.org/10.5194/egusphere-2026-353
Preprint. Discussion started: 28 January 2026
© Author(s) 2026. CC BY 4.0 License.

2.2 Trends in land carbon cycle datasets (TRENDY) models

The TRENDY dataset, an ensemble of DGVMs, provides estimates of terrestrial carbon sinks and sources (Sitch et al., 2024; Friedlingstein et al., 2024). We analyzed TRENDY outputs to identify changes in carbon flux sensitivity within East Asia, using 12 DGVMs included in the TRENDY version 13 ensemble (TRENDY v13) (Table 1) conducted for the Global Carbon Budget 2024 (Friedlingstein et al., 2024). We examined 8 ecosystem variables from TRENDY under the S3 scenario for 1959 to 2023, which considers changes of CO_2, climate, Land Use and Land Cover Change (Sitch et al., 2024). These variables include CO_2 fluxes (for example, GPP, autotrophic respiration (R_a), heterotrophic respiration (R_h)), water fluxes (for example, SM, transpiration, precipitation), and radiation including PAR. PAR was estimated as 0.5 of surface downwelling shortwave radiation, and values in W m^{-2} were converted to μmol s^{-1} m^{-2} using relationship 1 J = 4.6 μmol of PAR (Li et al., 2018). All datasets were regridded to a 1.0° × 1.0° spatial resolution using bilinear interpolation with the Climate Data Operator.

Table 1. Information on the TRENDY v13 model list used in this study.

	Model	Modeling center	Reference
1	CLASSIC	Environment and Climate Change Canada	(Asaadi and Arora, 2021)
2	CLM6.0	National Center for Atmospheric Research NCAR	(Lawrence et al., 2019)
3	E3SM	US Department of Energy	(Tang et al., 2023)
4	EDv3	University of Maryland	(Ma et al., 2021)
5	IBIS	McGill University	(Landry et al., 2016)
6	ISBA-CTRIP	Météo-France, French national meteorological centre	(Decharme et al., 2019)
7	JULES	UK Met Office, Centre for Ecology & Hydrology, University of Reading, University of Exeter	(Burton et al., 2019)
8	LPJmL	Potsdam Institute for Climate Impact Research	(Beer et al., 2007; Rolinski et al., 2018)
9	LPX-Bern	University of Bern	(Lienert and Joos, 2018)
10	ORCHIDEE	Institut Pierre-Simon Laplace, IPSL	(Krinner et al., 2005)
11	SDGVM	University of Sheffield	(Walker et al., 2017)
12	VISIT	The University of Tokyo, NIES, and JAMSTEC	(Ito, 2019)

https://doi.org/10.5194/egusphere-2026-353
Preprint. Discussion started: 28 January 2026
© Author(s) 2026. CC BY 4.0 License.

2.3 Cloud cover data

In TRENDY, DGVMs use forcing from the Climate Research Unit (CRU) dataset or from a combined product that integrates CRU with the Japanese 55-year Reanalysis (JRA-55) (Friedlingstein et al., 2024; Sitch et al., 2024). Because cloud cover is not provided in the TRENDY, we additionally used the CRU Time-series version 4.09 dataset to analyze cloud cover in this study.

2.4 Land cover data

The Moderate Resolution Imaging Spectroradiometer land cover type product is used to describe annual global land cover map at 500m spatial resolution (He et al., 2022a; Friedl and Sulla-Menashe, 2022). The dataset classifies each grid cell into 17 land cover classes based on International Geosphere-Biosphere Program schemes (Loveland and Belward, 1997; Zhang and Roy, 2017). We analyzed the mean land cover map for 2001 to 2023. If several land cover types appear with the same frequency within a grid cell, the type from the most recent year was used. The dataset was regridded to a 0.5° × 0.5° spatial resolution, with each grid cell used as the most frequently appearing land cover type within its extent, and no equal frequency was found.

2.5 Definition of sensitivity of ecosystem variables to Atmospheric CO_2 growth rate

Using Global Carbon Budget 2024 and TRENDY v13, we focused on assessing the sensitivity of ecosystem variables to ACGR from 1959 to 2023, over East Asia (10°-50° N, 90°-150° E). We adopted the methodology to define the sensitivity of GPP to global ACGR following (Li et al., 2024). The methods are as follows: First, the long-term trends of annual GPP and ACGR were removed to produce detrended time series (Fig. 1a, b). A linear regression was then performed using a 20-year moving window, with the slope of each regression defined as the sensitivity of GPP to ACGR (Fig. 1c). This represents the change in GPP in response to changes in ACGR, and a positive sensitivity indicates that GPP increases with an increase of ACGR and vice versa. In contrast, a negative sensitivity indicates either a decrease of GPP with an increase of ACGR or an increase of GPP with a decrease of ACGR. A value close to zero indicates a minimal or no response.

https://doi.org/10.5194/egusphere-2026-353
Preprint. Discussion started: 28 January 2026
© Author(s) 2026. CC BY 4.0 License.

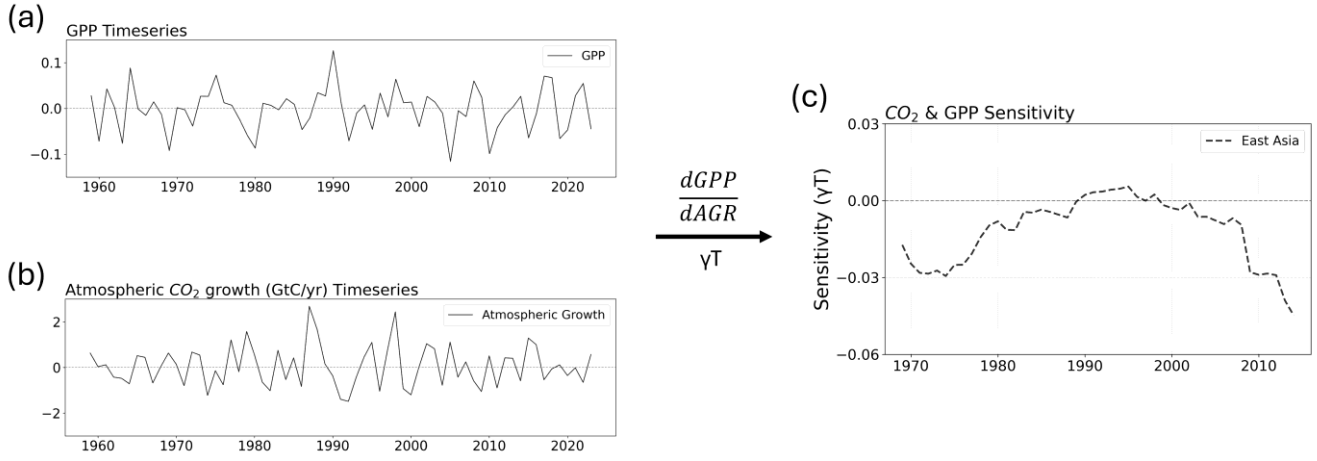

Figure 1. Methodological procedure for ecosystem productivity sensitivity to atmospheric CO_2 growth. (a) Detrended time series of GPP over East Asia from nine TRENDY v13 models. (b) Detrended atmospheric CO_2 growth from the Global Carbon Budget 2024. (c) Sensitivity of atmospheric CO_2 growth and GPP over 20-year moving windows in 1959-2023. For all panels, see Data and Methods for details.

On the other hand, NEP is an important indicator of the carbon sequestration capacity of terrestrial ecosystems (Yuan et al., 2023; Zhang et al., 2023) and was defined as GPP minus R_a and R_h [g m^{-2} day^{-1}].

$$NEP = GPP - R_a - R_h \quad (1)$$

PAR is essential energy source for vegetation photosynthesis (Ren et al., 2018; Kalaji et al., 2014), and as it is governed by atmospheric conditions rather than ACGR changes, it was analyzed using actual PAR values instead of ACGR sensitivity. Note that the same method to calculate the GPP sensitivity was applied to obtain the sensitivity of NEP, R_a, and SM in response to changes in ACGR.

3 Results

3.1 East Asian GPP and NEP relationship with ACGR

We first analyzed the sensitivity of NEP using each of the 12 DGVMs (Fig. 2a). All models except LPX-Bern simulated negative NEP sensitivities, suggesting a weakening of ecosystem carbon uptake ability in East Asia as ACGR increases for 1959-2023. Note that the statistical significance of NEP sensitivity was assessed using the last 20-year (2004-2023) moving window to reflect recent ecosystem changes. With these criteria applied, three models showed statistically insignificant relationships ($p>0.05$) or inconsistent signs; consequently, in subsequent analysis, only the nine models simulated as

https://doi.org/10.5194/egusphere-2026-353
Preprint. Discussion started: 28 January 2026
© Author(s) 2026. CC BY 4.0 License.

significant were used. The model selection was based on NEP sensitivity, as NEP is an integrated indicator accounting for both carbon uptake through photosynthesis and carbon release through respiration. Note that the overall results in the present study little change when all 12 DGVMs are used.

Following this selection, we analyzed the spatial distribution of GPP sensitivity in East Asia (Fig. 2b). Within East Asia, GPP sensitivity displays a distinct spatial contrast between central-eastern China, Korea, and Japan (Fig. 2b). This suggests that the response of ecosystem productivity (i.e., GPP sensitivity) to ACGR is not spatially consistent in East Asia and is influenced by regional environmental factors. Therefore, we separated East Asian into two regions to investigate the regional heterogeneity of ecosystem responses, one is East Asian monsoon region (10°-40° N, 110°-140° E) (Li and Zeng, 2002; Jianping and Qingcun, 2003) and the other is non-monsoon region – consisting of northern (41°-50° N, 90°-150° E) and western (10°-40° N, 90°-110° E) areas. Although the GPP sensitivity patterns do not perfectly align with the East Asian monsoon boundary, the monsoon region generally covers areas where positive sensitivity predominates, whereas the non-monsoon region includes areas with distinctly negative sensitivity. These regional distinctions, related to the monsoon system, provide a basis for understanding regional differences in ecosystem responses, reflecting the climatic influences of East Asia.

https://doi.org/10.5194/egusphere-2026-353
Preprint. Discussion started: 28 January 2026
© Author(s) 2026. CC BY 4.0 License.

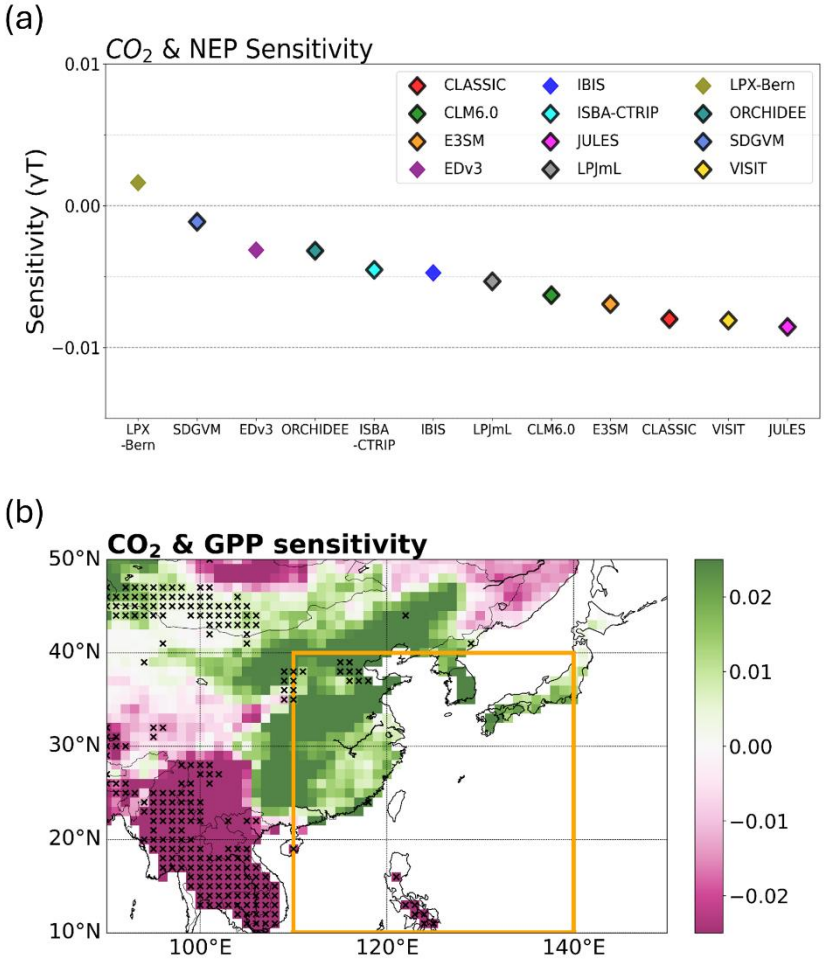

130 **Figure 2. (a) Scatter plot of the sensitivity between atmospheric CO_2 growth and NEP during 1959-2023, based on 12 models from TRENDY v13. Each scatter represents atmospheric CO_2 growth and NEP sensitivity of an individual model. Models with statistically significant relationships at the 95% confidence level (from the last 20-year window) are outlined in black. (b) Spatial patterns of the sensitivity to atmospheric CO_2 growth and GPP over East Asia, based on nine TRENDY models ensemble mean during 1959-2023. An x mark denotes statistically significant**
135 **relationships at the 90% confidence level evaluated from the last 20-year window.**

In Figure 3a, NEP sensitivity in non-monsoon region remained negative throughout the entire period, displaying an increasing trend until the late 1990s before decreasing. In contrast, the monsoon region showed weakly positive NEP sensitivity, which gradually decreased and became negative around the 1990s (Fig. 3a). Both regions exhibited a persistent
140 downward trend in negative NEP sensitivity, highlighting a greater weakening of carbon absorption capacity to an increase

https://doi.org/10.5194/egusphere-2026-353
Preprint. Discussion started: 28 January 2026
© Author(s) 2026. CC BY 4.0 License.

of ACGR in East Asia in recent decades. Similarly, the GPP sensitivity broadly revealed a similar pattern to NEP sensitivity, though with greater amplitude, indicating a stronger response to ACGR (Fig. 3b). In non-monsoon region, GPP sensitivity remained negative for most of the period, increasing until the late 1990s before declining (Fig. 3b). By contrast, the monsoon region showed positive GPP sensitivity that gradually weakened and turned negative in the late 2000s (Fig. 3b). This reduction in negative GPP sensitivity implies a progressive weakening of the vegetation response to ACGR over time. Particularly in non-monsoon region, the stronger magnitude of negative GPP sensitivity indicates that carbon uptake through photosynthesis is comparatively more constrained.

Furthermore, R_a sensitivity exhibited a pattern generally consistent with GPP sensitivity, as R_a is closely related to photosynthesis activity (Fig. 3c). Regarding these relationship, R_a showed a consistent decreasing trend with GPP sensitivity, reflecting a reduction in vegetation respiration activity associated with weakened photosynthetic response to ACGR.

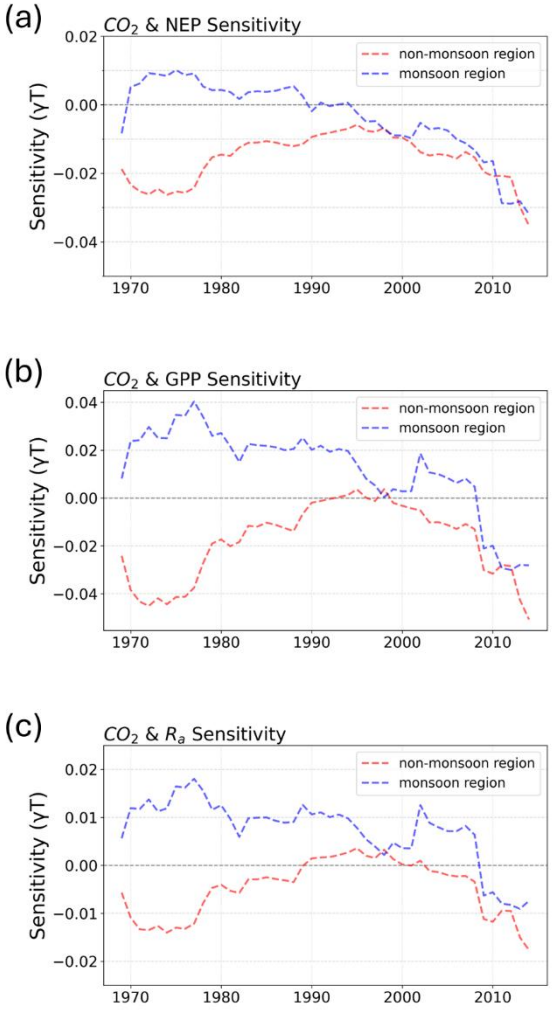

https://doi.org/10.5194/egusphere-2026-353
Preprint. Discussion started: 28 January 2026
© Author(s) 2026. CC BY 4.0 License.

Figure 3. Time series of the sensitivity between atmospheric CO_2 growth and (a) NEP, (b) GPP, (c) R_a over 20-year moving window in 1959-2023 (see Data and Methods for details). Lines show the ensemble mean of nine TRENDY models for the non-monsoon (red) and monsoon (blue) regions.

155

3.2 Regional and structural drivers of GPP sensitivity

While NEP represents a comprehensive result by including both photosynthetic production and respiratory losses, whereas GPP reflects only direct vegetation responses through photosynthesis. Therefore, GPP is more suitable for assessing changes in ecosystem productivity. The differences in GPP sensitivity between the monsoon and the non-monsoon regions are likely 160 attributable to differences in ecosystem structure, such as climate and hydrological conditions. To identify how these structural differences influence ecosystem productivities, we examined the relationships between GPP sensitivity and key environmental factors in each region (Fig. 4).

In the non-monsoon region, GPP sensitivity exhibited a strong positive correlation ($r=0.85$; here r is a simultaneous correlation with $p< 0.01$; Fig. 4a) with SM sensitivity. Both GPP and SM sensitivities showed an increase followed by a 165 decline over period, yet remained within the negative sensitivity range for most of the period (Fig. 4a). This indicates that the response of both variables to ACGR has consistently weakened. Additionally, the strong positive correlation suggests that the decline in SM sensitivity reflects reduced water availability that limits vegetation activity, ultimately leading to a decrease in GPP sensitivity. However, the monsoon region shows a contrasting pattern, resulting in a significant negative correlation ($r=-0.65$, $p<0.01$; Fig. 4b). In this region, SM sensitivity increased over time from negative to positive, while 170 GPP sensitivity decreased from positive to negative (Fig. 4b). Although an increase in SM sensitivity is generally associated with improved water availability and stomatal regulation, the GPP response to ACGR was weaken despite this improvement. This implies that the monsoon region is inherently a better-watered environment, meaning that increases in SM sensitivity no longer act as a primary constraint on GPP response. Consistent with this interpretation, the explanatory power of the relationship between SM and GPP sensitivities was remarkably lower in the monsoon region ($r^2=0.42$) compared with the 175 non-monsoon region ($r^2=0.72$), indicating that other environmental factors may play a key role.

To evaluate this possibility, we analyzed light, a crucial factor for photosynthesis. In the non-monsoon region, no meaningful relationship was observed between PAR and GPP sensitivity ($r=0.07$, $p>0.1$; Fig. 4c), consistent with the fact that PAR showed only minimal temporal variations, explaining no influence on GPP sensitivity ($r^2=0.01$; Fig. 4c). In the monsoon region, GPP sensitivity decreased from positive to negative, and PAR also showed a distinct decreasing trend (Fig. 180 4d); a significant positive correlation was shown ($r=0.72$, $p<0.01$; Fig. 4d). As sufficient radiation is required for vegetation to respond to ACGR, reduced PAR likely contributed to the weakening of GPP sensitivity, explained by high explanatory power ($r^2=0.52$; Fig. 4d). These results demonstrate that in the monsoon region, where moisture is relatively abundant, radiation limitation-rather than changes in SM sensitivity-plays a primary role in driving the reduction in GPP sensitivity.

https://doi.org/10.5194/egusphere-2026-353
Preprint. Discussion started: 28 January 2026
© Author(s) 2026. CC BY 4.0 License.

In the non-monsoon region, a significant positive correlation ($r=0.59$, $p<0.01$; Fig. 4e) was observed between transpiration sensitivity and SM sensitivity. Transpiration sensitivity increased from negative to slightly positive value before declining again, while SM sensitivity exhibited a similar increase-decrease pattern, but remained negative (Fig. 4e). This indicates that although ACGR causes stomatal closure, leads to reduced transpiration, such change does not translate into substantial SM accumulation in this comparatively dry region. Limited improvement in water availability, combined with reduced stomatal conductance, constrains photosynthetic activity, and contributes to the weakening of GPP sensitivity. In contrast, the monsoon region showed increasing SM sensitivity from negative to positive, whereas transpiration sensitivity exhibited a decreasing trend from positive to negative ($r=0.66$, $p<0.01$; Fig. 4f). These opposing trends reflect the physiological process whereby reduced stomatal conductance under ACGR suppresses transpiration, thereby promoting SM accumulation. In this relatively moisture-sufficient region, stomatal closure leads to increased SM; however, the simultaneous decrease in stomatal conductance limits the uptake of CO_2 required for photosynthesis, resulting in a weakening of GPP sensitivity. Consequently, GPP sensitivity in the monsoon region is influenced more strongly by PAR, while stomatal responses to ACGR contribute to reduction in vegetation productivity.

https://doi.org/10.5194/egusphere-2026-353
Preprint. Discussion started: 28 January 2026
© Author(s) 2026. CC BY 4.0 License.

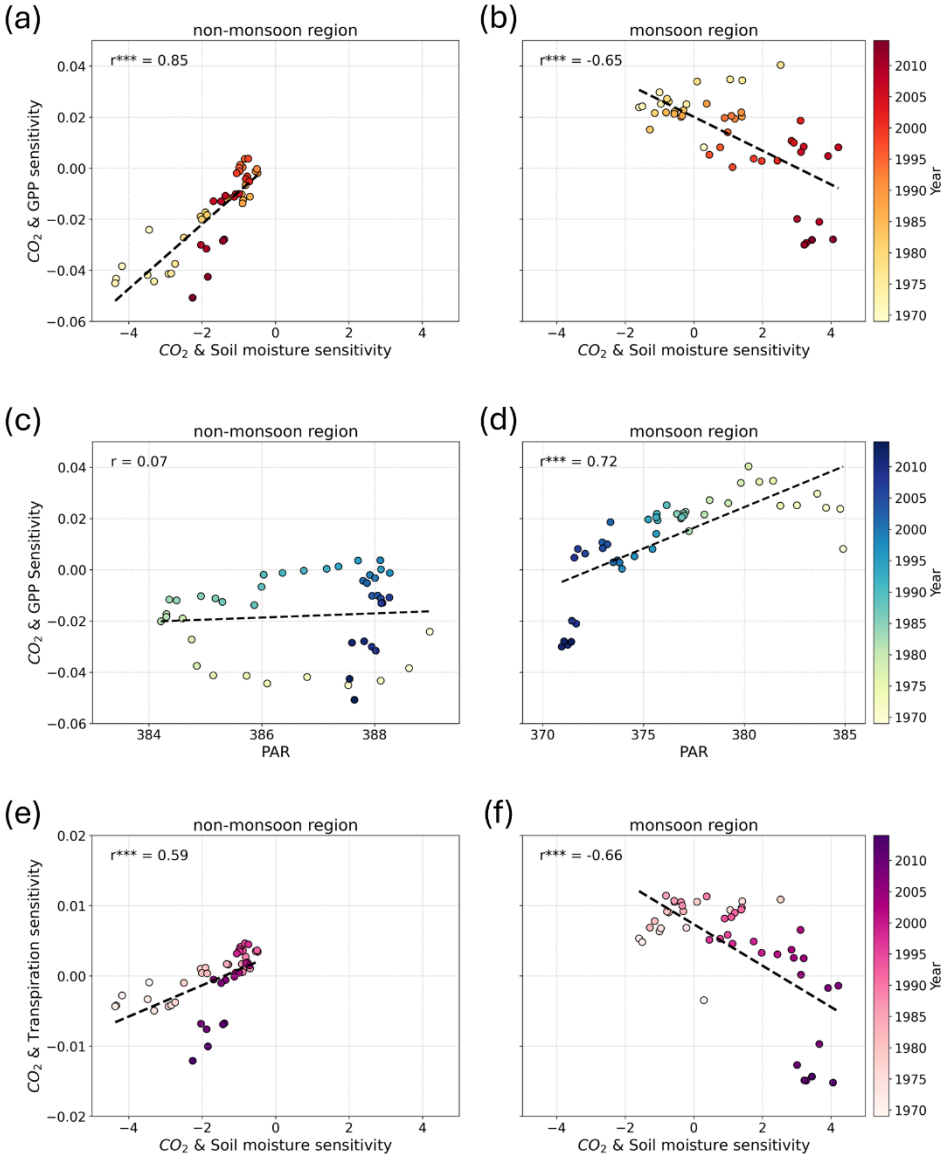

Figure 4. Correlation between (a, b) CO_2&GPP sensitivity (y-axis) and CO_2&SM sensitivity (x-axis), (c, d) CO_2&GPP sensitivity (y-axis) and PAR (x-axis), and (e, f) CO_2&transpiration sensitivity (y-axis) and CO_2&SM sensitivity (x-axis) for the non-monsoon (left) and monsoon (right) region during 1959-2023. Each scatter represents a 20-year moving window, with color changes representing the time period. ***p < 0.01; **p < 0.05; *p < 0.1; not significant, p > 0.1.

https://doi.org/10.5194/egusphere-2026-353
Preprint. Discussion started: 28 January 2026
© Author(s) 2026. CC BY 4.0 License.

3.3 Temporal change of environmental controls on GPP sensitivity

As shown in Figure 3b, the GPP sensitivity in non-monsoon region showed a reversal pattern, increasing until 1998 before decreasing. To better understand this pattern, the relationship between GPP sensitivity and environmental factors was reanalyzed for two periods, i.e., 1959- 1998 and 1999-2023 (Fig. 5, 6), using the same approach as in Figure 4.

In non-monsoon region, the correlation between GPP sensitivity and SM sensitivity exhibited a strong positive correlation in both periods ($r=0.92$, $p<0.01$ for the early period; $r=0.87$, $p<0.01$ for the late period), with high explanatory power ($r^2=0.85$ and $r^2=0.76$, respectively; Fig. 5a, b). This follows the same pattern as the relationship between GPP sensitivity and SM sensitivity observed in the entire period, suggesting that SM sensitivity remained the key factor regulating the GPP response to ACGR throughout the study period. Conversely, the role of radiation showed temporal shifts. During the early period, GPP sensitivity showed no correlation with PAR ($r=0.09$, $p>0.1$; Fig. 5c), consistent with the full period analysis. However, in the late period, a positive correlation emerged ($r=0.59$, $p<0.05$; $r^2=0.35$; Fig. 5d), with both PAR and GPP sensitivity decreasing, and GPP sensitivity having a negative value. This reveals that while SM remained the main factor, the increased coefficient of determination in the later period implies that radiation limitation influences vegetation productivity response to ACGR as a regulating factor. In addition, the relationship between transpiration sensitivity and SM sensitivity also remained consistently a positive correlation in both periods ($r=0.89$, $p<0.01$ for the early period; $r=0.85$, $p<0.01$ for the late period), with consistently high coefficients of determination ($r^2=0.80$ and $r^2=0.73$, respectively; Fig. 5e, f). Both sensitivities increased during the initial period before decreasing later on, reflecting the same mechanism identified in the analysis of the overall period. That is, the reduction in stomatal conductance response to ACGR suppresses transpiration but does not lead to a substantial increase in SM under relatively dry conditions. Simultaneously, it limits vegetation CO_2 uptake, resulting in a weakening of GPP sensitivity.

https://doi.org/10.5194/egusphere-2026-353
Preprint. Discussion started: 28 January 2026
© Author(s) 2026. CC BY 4.0 License.

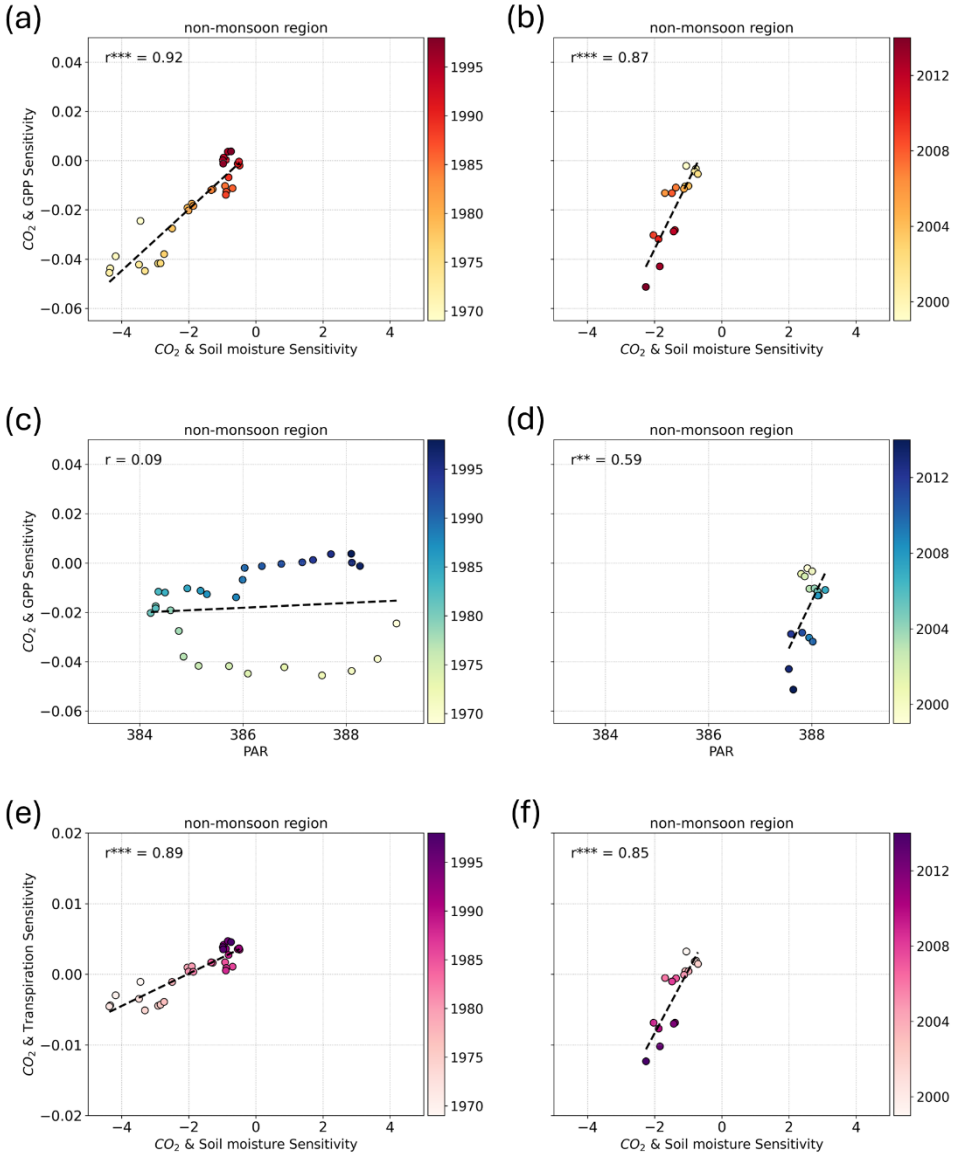

Figure 5. Correlation between (a, b) CO_2&GPP sensitivity (y-axis) and CO_2&SM sensitivity (x-axis), (c, d) CO_2&GPP sensitivity (y-axis) and PAR (x-axis), and (e, f) CO_2&transpiration sensitivity (y-axis) and CO_2&SM sensitivity (x-axis) for the non-monsoon region during 1959-1998 (left) and 1999-2023 (right). Each scatter represents a 20-year moving window, with color changes representing the time period. ***p < 0.01; **p < 0.05; *p < 0.1; not significant, p > 0.1.

In monsoon region, the correlation between GPP sensitivity and SM sensitivity became slightly stronger during the late period, though it remains statistically insignificant in both periods (r=0.01, p>0.1 for the early period; r=-0.30, p>0.1 for the

https://doi.org/10.5194/egusphere-2026-353
Preprint. Discussion started: 28 January 2026
© Author(s) 2026. CC BY 4.0 License.

late period; Fig. 6a, b). Compared to the analysis across the entire period, most environmental relationships showed weaker correlations when analyzed by separated period, with the exception of the relationship between GPP sensitivity and PAR. The relationship between GPP sensitivity and PAR exhibited a significant positive correlation in both periods ($r=0.46$, $p<0.05$ for the early period; $r=0.77$, $p<0.01$ for the late period), and its coefficients of determination strengthened over time ($r^2=0.21$ and $r^2=0.59$, respectively; Fig. 6c, d), emphasizing that the role of PAR in explaining GPP sensitivity enhanced during later period. The relationship between transpiration sensitivity and SM sensitivity showed insignificant correlation during early period ($r=0.13$, $p>0.1$; Fig.6e), but became significantly negatively correlated during the later period ($r=-0.50$, $p<0.05$; $r^2=0.26$; Fig. 6f), highlighting that the same pattern identified in the full period analysis whereby reduced stomatal conductance in response to ACGR suppresses transpiration and accelerates SM accumulation. In conclusion, the coefficient of determination for the entire period indicates that the primary factor weakening GPP sensitivity is the reduction in PAR. Moreover, although no clear relationship emerged during the early period, the decrease in stomatal conductance in response to ACGR promotes SM accumulation while simultaneously constraining vegetation CO_2 uptake, thereby contributing to the weakening of GPP sensitivity.

https://doi.org/10.5194/egusphere-2026-353
Preprint. Discussion started: 28 January 2026
© Author(s) 2026. CC BY 4.0 License.

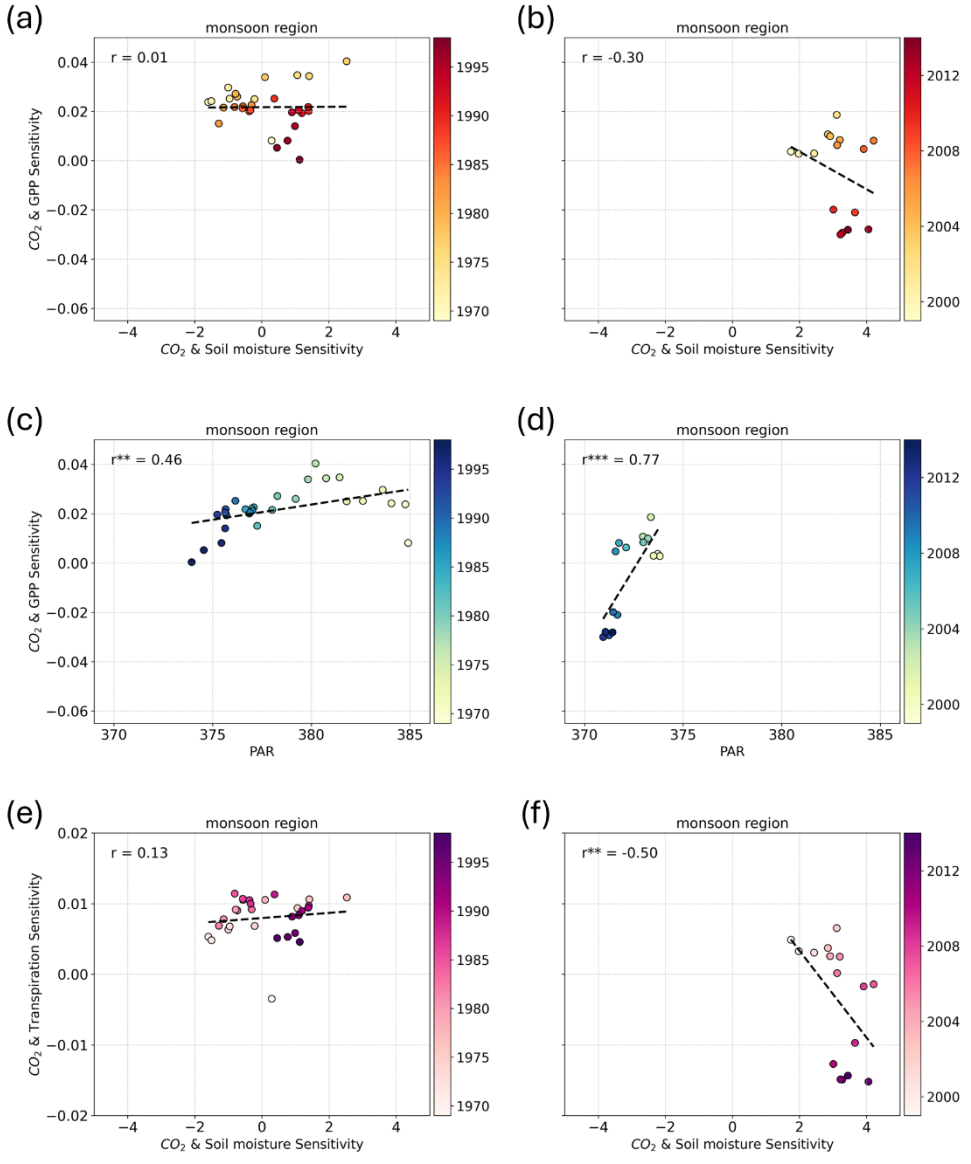

Figure 6. Correlation between (a, b) CO_2&GPP sensitivity (y-axis) and CO_2&SM sensitivity (x-axis), (c, d) CO_2&GPP sensitivity (y-axis) and PAR (x-axis), and (e, f) CO_2&transpiration sensitivity (y-axis) and CO_2&SM sensitivity (x-axis) for the monsoon region during 1959-1998 (left) and 1999-2023 (right). Each scatter represents a 20-year moving window, with color changes representing the time period. ***p < 0.01; **p < 0.05; *p < 0.1; not significant, p > 0.1.

Furthermore, variations in PAR are connected to changes in atmospheric conditions, including precipitation and cloud cover, within East Asia. In the non-monsoon region, while precipitation trends are not statistically significant (slope=0.0001),

https://doi.org/10.5194/egusphere-2026-353
Preprint. Discussion started: 28 January 2026
© Author(s) 2026. CC BY 4.0 License.

cloud cover (slope=-0.058, p<0.01) and PAR (slope=0.056, p<0.01) exhibit significant changes (Fig. 7a, c, e). The correlation between precipitation and cloud cover is close to zero (r=-0.08, p>0.1), indicating a weak association between precipitation and cloud formation processes. This may also be linked to the relatively low precipitation levels in the non-monsoon region. However, a distinct negative correlation emerges between cloud cover and PAR (r=-0.78, p<0.01), with decreased (increased) cloud cover reducing the amount of shortwave radiation reaching the surface, thereby increasing (decreasing) PAR. More prominently, in the monsoon region, PAR shows a consistent downward trend (slope=-0.286, p<0.01), while precipitation (slope=0.003, p<0.01) and cloud cover (slope=0.020, p<0.01) generally increase (Fig. 7b, d, f). Precipitation and cloud cover exhibit a significant positive correlation (r=0.77, p<0.01), possibly reflecting that increased precipitation provides favorable environmental conditions for cloud formation. Conversely, cloud cover and PAR show a strong negative correlation (r=-0.91, p<0.01), consistent with the general mechanism whereby increased cloud cover reduces shortwave radiation. A reduction in PAR limits the light available for photosynthesis, leading to decreased vegetation productivity. Consequently, the reduced GPP sensitivity in monsoon region indicates that even when SM is abundant, the ecosystem's carbon absorption capacity may still be constrained if radiation is limited by precipitation and cloud cover.

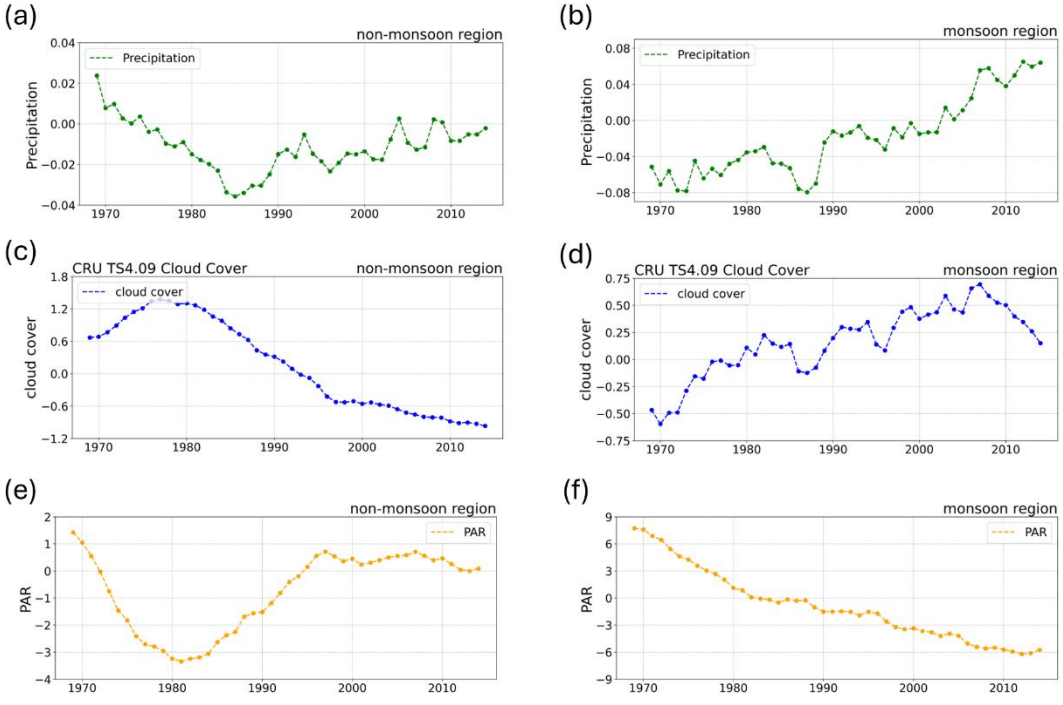

Figure 7. Time series of the (a, b) Precipitation, (c, d) Cloud cover, (e, f) PAR anomalies over 20-year moving window in 1959-2023. Panels (a), (b), (e), and (f) are based on the ensemble mean of nine TRENDY models, and cloud cover in panels (c) and (d) is derived from CRU TS dataset.

https://doi.org/10.5194/egusphere-2026-353
Preprint. Discussion started: 28 January 2026
© Author(s) 2026. CC BY 4.0 License.

4 Discussion

Vegetation composition in East Asia exhibits distinct spatial heterogeneity even within non-monsoon and monsoon regions, which contributes to structural and functional characteristics of terrestrial ecosystem. As ecosystem productivity is affected by vegetation type, understanding the mechanisms underlying regional differences in ACGR and GPP relationship is essential. Therefore, we examined East Asian land cover based on MODIS dataset. Our analysis revealed that the non-monsoon region dominated by grasslands and barren, while monsoon region predominantly features croplands and woody savannas (Fig. 8). Generally, ecosystems dominated by croplands and woody savannas maintain higher vegetation productivity compared with grasslands and barren areas. These differences in vegetation structure may help explain the pattern where positive GPP sensitivity was observed initially in the monsoon region, whereas negative sensitivity was maintained for most of the period in the non-monsoon region. This sustained negative sensitivity is likely a consequence of stress factors being reflected more rapidly in the non-monsoon region, depending on vegetation structure. Consequently, these variations imply different ecosystem functions and vegetation-moisture mechanisms across regions, emphasizing that regional environmental conditions control ecosystem productivity responses to ACGR.

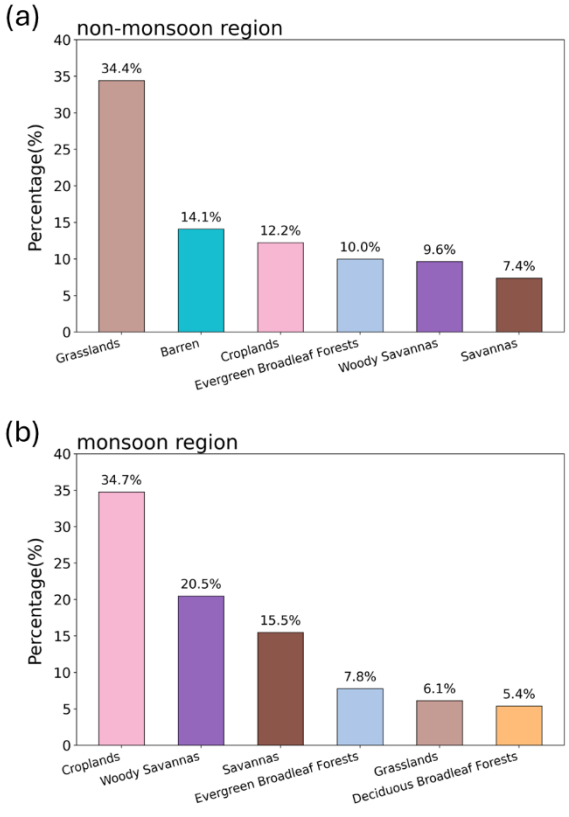

https://doi.org/10.5194/egusphere-2026-353
Preprint. Discussion started: 28 January 2026
© Author(s) 2026. CC BY 4.0 License.

Figure 8. East Asian land cover distribution based on IGBP classification. MODIS land cover averaged during 2001-2023, percentage distribution of land cover types in (a) non-monsoon and (b) monsoon region. For all panels, see Data and Methods for details.

5 Conclusion

We investigated the mechanisms regulating ecosystem productivity across different regions within East Asia based on the spatial pattern of GPP sensitivity. The analysis focused on moisture and light conditions, as well as stomatal responses, which can influence GPP sensitivity. These factors were interpreted considering the climatic characteristics of monsoon and non-monsoon regions. Furthermore, based on the diverse vegetation types distributed across East Asia, the factors contributing to changes in GPP sensitivity were additionally analyzed. The main conclusions were as follows:

(1) GPP sensitivity was negative in non-monsoon and positive in monsoon regions. However, both regions ultimately showed a decline trend, converging towards negative sensitivity as the time progresses. This trend was also observed in NEP sensitivity, indicating a weakening of ecosystem productivity and carbon sequestration in East Asia.

(2) In the non-monsoon region, SM sensitivity consistently appeared as the dominant factor constraining GPP sensitivity, whereas in the monsoon region, reductions in PAR played the primary role in weakening the GPP response. Across both regions, reduced stomatal conductance under ACGR limited vegetation CO_2 uptake, acting as a common mechanism that converged over time towards a weakening of GPP sensitivity.

(3) Regional differences in moisture conditions were also revealed in stomatal responses. In non-monsoon region, reduced transpiration did not lead to SM accumulation, whereas in the relatively humid monsoon region, the same stomatal response contributed to SM accumulation.

Our findings provide important implications for projecting future carbon cycle under climate change. The weakening sensitivity of ecosystem productivity to ACGR suggests that the CO_2 effect on East Asian vegetation is saturating or even declining, which potentially accelerates global warming through a reduced terrestrial carbon sink. Therefore, future climate projections and carbon budget assessments need to explicitly account for regional climatic constraints, particularly soil moisture and radiation. Overall, these results highlight that future changes in carbon uptake across East Asia will be determined not only by rising CO_2 but also by climatic factors, implying that carbon neutrality strategies should be designed with regional specificity influenced by internal climate variability.

https://doi.org/10.5194/egusphere-2026-353
Preprint. Discussion started: 28 January 2026
© Author(s) 2026. CC BY 4.0 License.

Code and data availability

The sensitivity analysis code of this study is available via Zenodo at https://zenodo.org/records/18307449. The sensitivity calculation follows the method of Li et al., (2024), with minor modifications. Additionally, we used LOWESS-based trend removal using A. Gramfort's python package (https://gist.github.com/agramfort/850437). (1) The dynamic global vegetation models outputs from TRENDY v13 are available upon request. (2) The cloud cover data used in this study was obtained from the CRU TS version 4.09 dataset, provided by the Center for Environmental Data Analysis (CEDA), and are available at https://data.ceda.ac.uk/badc/cru/data/cru_ts/cru_ts_4.09/data/cld. (3) The MODIS land-cover data was obtained from the MCD12Q1 version 6.1 data, available from NASA Earthdata at DOI: https://doi.org/10.5067/MODIS/MCD12Q1.061. The data was accessed via the AppEEARS.

Author contributions

YSN: Data analysis, Conceptualization, Writing-original draft. SWY: Supervision, Conceptualization, Writing-review and editing. JSK: Writing-review and editing.

Competing interests

The authors declare that they have no conflict of interest.

Acknowledgements

This work is supported by the Korea Environment Industry and Technology Institute (KEITI) through Climate Change R&D Project for New Climate Regime funded by Korea Ministry of Environment (MOE) (2022003560001).We are sincerely grateful to the TRENDY team for developing and providing the Dynamic Global Vegetation Models dataset used in this study.

References

Asaadi, A. and Arora, V. K.: Implementation of nitrogen cycle in the CLASSIC land model, Biogeosciences, 18, 669-706, https://doi.org/10.5194/bg-18-669-2021, 2021.

https://doi.org/10.5194/egusphere-2026-353
Preprint. Discussion started: 28 January 2026
© Author(s) 2026. CC BY 4.0 License.

Baldocchi, D., Ryu, Y., and Keenan, T.: Terrestrial carbon cycle variability, F1000Research, 5, https://doi.org/10.12688/f1000research.8962.1, 2016.

Beer, C., Lucht, W., Gerten, D., Thonicke, K., and Schmullius, C.: Effects of soil freezing and thawing on vegetation carbon density in Siberia: A modeling analysis with the Lund-Potsdam-Jena Dynamic Global Vegetation Model (LPJ-DGVM), Glob. Biogeochem. Cycle, 21, https://doi.org/10.1029/2006GB002760, 2007.

Bi, W., He, W., Zhou, Y., Ju, W., Liu, Y., Liu, Y., Zhang, X., Wei, X., and Cheng, N.: A global 0.05 dataset for gross primary production of sunlit and shaded vegetation canopies from 1992 to 2020, Scientific Data, 9, 213, https://doi.org/10.1038/s41597-022-01309-2, 2022.

Burton, C., Betts, R., Cardoso, M., Feldpausch, T. R., Harper, A., Jones, C. D., Kelley, D. I., Robertson, E., and Wiltshire, A.: Representation of fire, land-use change and vegetation dynamics in the Joint UK Land Environment Simulator vn4. 9 (JULES), Geosci. Model Dev., 12, 179-193, https://doi.org/10.5194/gmd-12-179-2019, 2019.

Canadell, J. G., Le Quéré, C., Raupach, M. R., Field, C. B., Buitenhuis, E. T., Ciais, P., Conway, T. J., Gillett, N. P., Houghton, R., and Marland, G.: Contributions to accelerating atmospheric CO2 growth from economic activity, carbon intensity, and efficiency of natural sinks, Proc. Natl. Acad. Sci., 104, 18866-18870, https://doi.org/10.1073/pnas.0702737104, 2007.

Decharme, B., Delire, C., Minvielle, M., Colin, J., Vergnes, J. P., Alias, A., Saint-Martin, D., Séférian, R., Sénési, S., and Voldoire, A.: Recent changes in the ISBA-CTRIP land surface system for use in the CNRM-CM6 climate model and in global off-line hydrological applications, J. Adv. Model. Earth Syst., 11, 1207-1252, https://doi.org/10.1029/2018MS001545, 2019.

Friedl, M. and Sulla-Menashe, D.: MODIS/Terra+Aqua Land Cover Type Yearly L3 Global 500m SIN Grid V061 (v061), NASA Land Processes Distributed Active Archive Center [data set], https://doi.org/10.5067/MODIS/MCD12Q1.061, 2022.

Friedlingstein, P., O'sullivan, M., Jones, M. W., Andrew, R. M., Hauck, J., Landschützer, P., Le Quéré, C., Li, H., Luijkx, I. T., and Olsen, A.: Global carbon budget 2024, Earth Syst. Sci. Data, 2024, 1-133, https://doi.org/10.5194/essd-17-965-2025, 2024.

Fu, C.: Potential impacts of human-induced land cover change on East Asia monsoon, Glob. Planet. Change, 37, 219-229, https://doi.org/10.1016/S0921-8181(02)00207-2, 2003.

Global Carbon Project: Supplemental data of Global Carbon Budget 2024 (Version 1.0) (v1.0), Global Carbon Project [data set], https://doi.org/10.18160/gcp-2024, 2024.

Han, M.-Y., Zhang, Y., and Peng, J.: How the enhanced East Asian summer monsoon regulates total gross primary production in eastern China, Adv. Clim. Chang. Res., 15, 244-252, https://doi.org/10.1016/j.accre.2024.04.001, 2024.

He, S., Li, J., Wang, J., and Liu, F.: Evaluation and analysis of upscaling of different land use/land cover products (FORM-GLC30, GLC_FCS30, CCI_LC, MCD12Q1 and CNLUCC): A case study in China, Geocarto Int., 37, 17340-17360, https://doi.org/10.1080/10106049.2022.2127926, 2022a.

https://doi.org/10.5194/egusphere-2026-353
Preprint. Discussion started: 28 January 2026
© Author(s) 2026. CC BY 4.0 License.

He, Y., Oh, J., Lee, E., and Kim, Y.: Land cover and land use mapping of the east Asian summer monsoon region from 1982 to 2015, Land, 11, 391, https://doi.org/10.3390/land11030391, 2022b.

Ito, A.: Disequilibrium of terrestrial ecosystem CO 2 budget caused by disturbance-induced emissions and non-CO 2 carbon export flows: a global model assessment, Earth Syst. Dynam., 10, 685-709, https://doi.org/10.5194/esd-10-685-2019, 2019.

Jianping, L. and Qingcun, Z.: A new monsoon index and the geographical distribution of the global monsoons, Adv. Atmos. Sci., 20, 299-302, https://doi.org/10.1007/s00376-003-0016-5, 2003.

Kalaji, H. M., Jajoo, A., Oukarroum, A., Brestic, M., Zivcak, M., Samborska, I. A., Cetner, M. D., Łukasik, I., Goltsev, V., and Ladle, R. J.: The use of chlorophyll fluorescence kinetics analysis to study the performance of photosynthetic machinery in plants, in: Emerging technologies and management of crop stress tolerance, edited by: Ahmad, P., and Rasool, S., Elsevier., 347-384, https://doi.org/10.1016/B978-0-12-800875-1.00015-6, 2014.

Keeling, C. D., Bacastow, R. B., Bainbridge, A. E., Ekdahl Jr, C. A., Guenther, P. R., Waterman, L. S., and Chin, J. F.: Atmospheric carbon dioxide variations at Mauna Loa observatory, Hawaii, Tellus, 28, 538-551, https://doi.org/10.3402/tellusa.v28i6.11322, 1976.

Kim, J. and Park, S.: Uncertainties in calculating precipitation climatology in East Asia, Hydrol. Earth Syst. Sci., 20, 651-658, https://doi.org/10.5194/hess-20-651-2016, 2016.

Krinner, G., Viovy, N., de Noblet-Ducoudré, N., Ogée, J., Polcher, J., Friedlingstein, P., Ciais, P., Sitch, S., and Prentice, I. C.: A dynamic global vegetation model for studies of the coupled atmosphere-biosphere system, Glob. Biogeochem. Cycle, 19, https://doi.org/10.1029/2003GB002199, 2005.

Lan, X., Tans, P., and Thoning, K. W.: Trends in globally-averaged CO2 determined from NOAA Global Monitoring Laboratory measurements (v2025-09), NOAA Global Monitoring Laboratory measurements [data set], https://doi.org/10.15138/9N0H-ZH07, 2025.

Landry, J.-S., Price, D. T., Ramankutty, N., Parrott, L., and Matthews, H. D.: Implementation of a Marauding Insect Module (MIM, version 1.0) in the Integrated BIosphere Simulator (IBIS, version 2.6 b4) dynamic vegetation–land surface model, Geosci. Model Dev., 9, 1243-1261, https://doi.org/10.5194/gmd-9-1243-2016, 2016.

Lawrence, D. M., Fisher, R. A., Koven, C. D., Oleson, K. W., Swenson, S. C., Bonan, G., Collier, N., Ghimire, B., Van Kampenhout, L., and Kennedy, D.: The Community Land Model version 5: Description of new features, benchmarking, and impact of forcing uncertainty, J. Adv. Model. Earth Syst., 11, 4245-4287, https://doi.org/10.1029/2018MS001583, 2019.

Li, J. and Zeng, Q.: A unified monsoon index, Geophys. Res. Lett., 29, 115-111-115-114, https://doi.org/10.1029/2001GL013874, 2002.

Li, L., Wang, Y., Arora, V. K., Eamus, D., Shi, H., Li, J., Cheng, L., Cleverly, J., Hajima, T., and Ji, D.: Evaluating global land surface models in CMIP5: Analysis of ecosystem water-and light-use efficiencies and rainfall partitioning, J. Clim., 31, 2995-3008, https://doi.org/10.1175/JCLI-D-16-0177.1, 2018.

https://doi.org/10.5194/egusphere-2026-353
Preprint. Discussion started: 28 January 2026
© Author(s) 2026. CC BY 4.0 License.

Li, N., Sippel, S., Linscheid, N., Rödenbeck, C., Winkler, A. J., Reichstein, M., Mahecha, M. D., and Bastos, A.: Enhanced global carbon cycle sensitivity to tropical temperature linked to internal climate variability, Sci. Adv., 10, eadl6155, https://doi.org/10.1126/sciadv.adl6155, 2024.

Lienert, S. and Joos, F.: A Bayesian ensemble data assimilation to constrain model parameters and land-use carbon emissions, Biogeosciences, 15, 2909-2930, https://doi.org/10.5194/bg-15-2909-2018, 2018.

Loveland, T. R. and Belward, A.: The IGBP-DIS global 1km land cover data set, DISCover: First results, Int. J. Remote Sens., 18, 3289-3295, https://doi.org/10.1080/014311697217099, 1997.

Ma, L., Hurtt, G., Ott, L., Sahajpal, R., Fisk, J., Lamb, R., Tang, H., Flanagan, S., Chini, L., and Chatterjee, A.: Global evaluation of the Ecosystem Demography model (ED v3. 0), Geosci. Model Dev., 2021, 1-41, https://doi.org/10.5194/gmd-15-1971-2022, 2021.

Madani, N., Parazoo, N. C., Kimball, J. S., Ballantyne, A. P., Reichle, R. H., Maneta, M., Saatchi, S., Palmer, P. I., Liu, Z., and Tagesson, T.: Recent amplified global gross primary productivity due to temperature increase is offset by reduced productivity due to water constraints, AGU Adv., 1, e2020AV000180, https://doi.org/10.1029/2020AV000180, 2020.

Na, Y.-S. and Yeh, S.-W.: Changes in vegetation-induced carbon sequestration in East Asia under global warming in CMIP6 Earth system models, Earth Syst. Environ., 1-16, https://doi.org/10.1007/s41748-025-00731-x, 2025.

Penuelas, J.: Decreasing efficiency and slowdown of the increase in terrestrial carbon-sink activity, One Earth, 6, 591-594, https://doi.org/10.1016/j.oneear.2023.05.013, 2023.

Ren, X., He, H., Zhang, L., and Yu, G.: Global radiation, photosynthetically active radiation, and the diffuse component dataset of China, 1981–2010, Earth Syst. Sci. Data, 10, 1217-1226, https://doi.org/10.5194/essd-10-1217-2018, 2018.

Rolinski, S., Müller, C., Heinke, J., Weindl, I., Biewald, A., Bodirsky, B. L., Bondeau, A., Boons-Prins, E. R., Bouwman, A. F., and Leffelaar, P. A.: Modeling vegetation and carbon dynamics of managed grasslands at the global scale with LPJmL 3.6, Geosci. Model Dev., 11, 429-451, https://doi.org/10.5194/gmd-11-429-2018, 2018.

Shin, M.-S., Yeh, S.-W., Lee, H.-J., and Park, C.-E.: Changes in the relationship between climate variables and vegetation carbon uptake in East Asia, Ecol. Inform., 103375, https://doi.org/10.1016/j.ecoinf.2025.103375, 2025.

Sitch, S., O'sullivan, M., Robertson, E., Friedlingstein, P., Albergel, C., Anthoni, P., Arneth, A., Arora, V. K., Bastos, A., and Bastrikov, V.: Trends and drivers of terrestrial sources and sinks of carbon dioxide: An overview of the TRENDY project, Glob. Biogeochem. Cycle, 38, e2024GB008102, https://doi.org/10.1029/2024GB008102, 2024.

Tang, Q., Golaz, J.-C., Van Roekel, L. P., Taylor, M. A., Lin, W., Hillman, B. R., Ullrich, P. A., Bradley, A. M., Guba, O., and Wolfe, J. D.: The fully coupled regionally refined model of E3SM version 2: Overview of the atmosphere, land, and river results, Geosci. Model Dev., 16, 3953-3995, https://doi.org/10.5194/gmd-16-3953-2023, 2023.

Ueyama, M., Iwata, H., Nagano, H., Kukuu, N., and Harazono, Y.: Anomalous wet summers and rising atmospheric CO2 concentrations increase the CO2 sink in a poorly drained forest on permafrost, Proc. Natl. Acad. Sci., 121, e2414539121, https://doi.org/10.1073/pnas.2414539121, 2024.

https://doi.org/10.5194/egusphere-2026-353
Preprint. Discussion started: 28 January 2026
© Author(s) 2026. CC BY 4.0 License.

Walker, A. P., Quaife, T., Van Bodegom, P. M., De Kauwe, M. G., Keenan, T. F., Joiner, J., Lomas, M. R., MacBean, N., Xu, C., and Yang, X.: The impact of alternative trait-scaling hypotheses for the maximum photosynthetic carboxylation rate (Vcmax) on global gross primary production, New Phytol., 215, 1370-1386, https://doi.org/10.1111/nph.14623, 2017.

Wang, S., Zhang, Y., Ju, W., Chen, J. M., Ciais, P., Cescatti, A., Sardans, J., Janssens, I. A., Wu, M., and Berry, J. A.: Recent global decline of CO2 fertilization effects on vegetation photosynthesis, Science, 370, 1295-1300, https://doi.org/10.1126/science.abb7772, 2020.

Wang, Z., Peñuelas, J., Tagesson, T., Smith, W., Wu, M., He, W., Sitch, S., and Wang, S.: Evolution of Global Terrestrial Gross Primary Productivity Trend, Ecosyst. Health Sustain., 10, 0278, https://doi.org/10.34133/ehs.0278, 2024.

Yuan, Z., Jiang, Q., and Yin, J.: Impact of climate change and land use change on ecosystem net primary productivity in the Yangtze River and Yellow River Source Region, China, Watershed Ecol. Environ., 5, 125-133, https://doi.org/10.1016/j.wsee.2023.04.001, 2023.

Yun, H., Tang, J., D'Imperio, L., Wang, X., Qu, Y., Liu, L., Zhuang, Q., Zhang, W., Wu, Q., and Chen, A.: Warming and increased respiration have transformed an alpine steppe ecosystem on the Tibetan Plateau from a carbon dioxide sink into a source, J. Geophys. Res.: Biogeosci., 127, e2021JG006406, https://doi.org/10.1029/2021JG006406, 2022.

Zhang, H. K. and Roy, D. P.: Using the 500 m MODIS land cover product to derive a consistent continental scale 30 m Landsat land cover classification, Remote Sens. Environ., 197, 15-34, https://doi.org/10.1016/j.rse.2017.05.024, 2017.

Zhang, X., Chen, Y., Zhang, Q., Xia, Z., Hao, H., and Xia, Q.: Potential evapotranspiration determines changes in the carbon sequestration capacity of forest and grass ecosystems in Xinjiang, Northwest China, Glob. Ecol. Conserv., 48, e02737, https://doi.org/10.1016/j.gecco.2023.e02737, 2023.